Accepted Manuscript

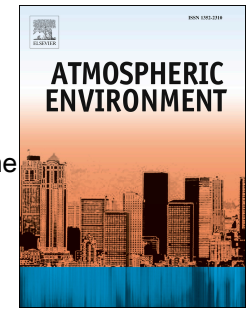

PM10 source apportionment applying PMF and chemical tracer analysis to ship-borne measurements in the Western Mediterranean

M.C. Bove, P. Brotto, G. Calzolai, F. Cassola, F. Cavalli, P. Fermo, J. Hjorth, D. Massabò, S. Nava, A. Piazzalunga, C. Schembari, P. Prati

PII: S1352-2310(15)30518-5

DOI: 10.1016/j.atmosenv.2015.11.009

Reference: AEA 14261

To appear in: *Atmospheric Environment*

Received Date: 10 July 2015

Revised Date: 3 November 2015

Accepted Date: 4 November 2015

Please cite this article as: Bove, M.C., Brotto, P., Calzolai, G., Cassola, F., Cavalli, F., Fermo, P., Hjorth, J., Massabò, D., Nava, S., Piazzalunga, A., Schembari, C., Prati, P., PM10 source apportionment applying PMF and chemical tracer analysis to ship-borne measurements in the Western Mediterranean, *Atmospheric Environment* (2015), doi: 10.1016/j.atmosenv.2015.11.009.

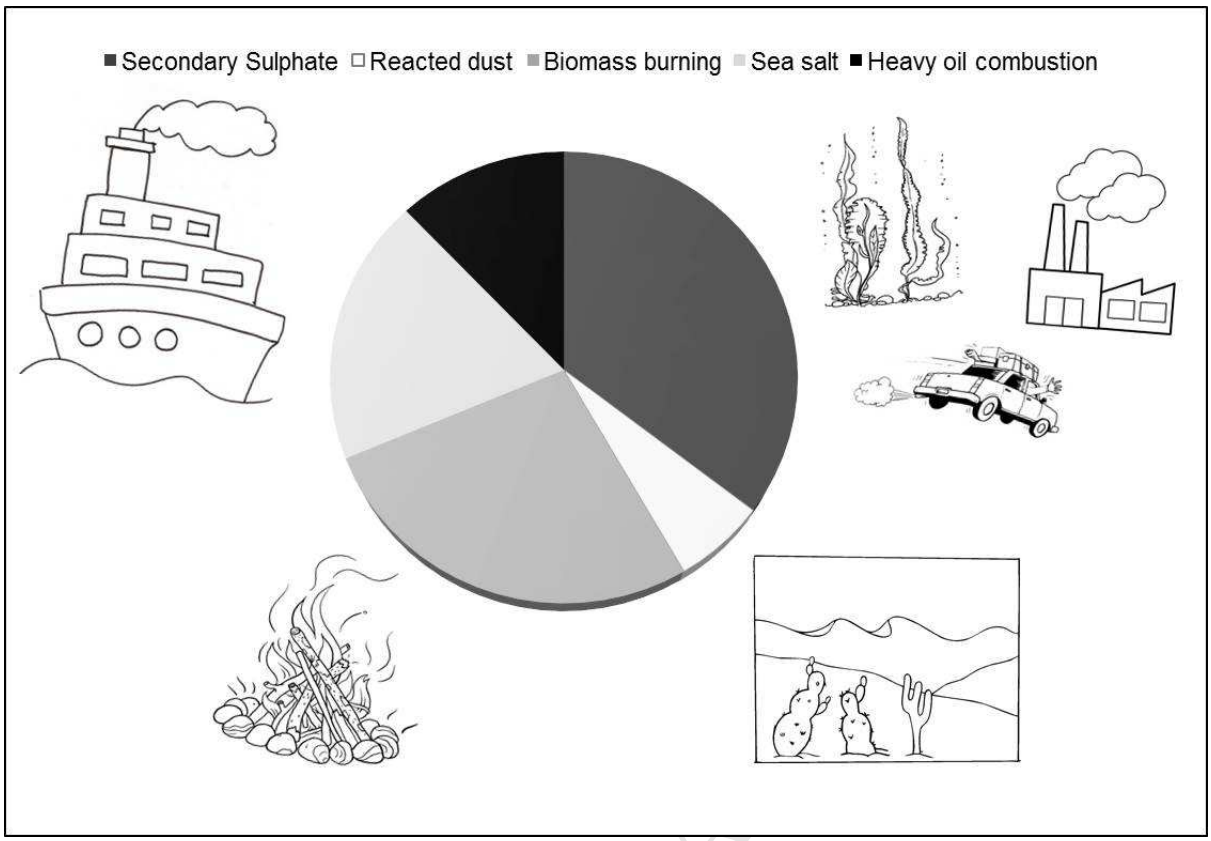

PM10 source apportionment applying PMF and chemical tracer analysis to ship-borne measurements in the Western Mediterranean

M.C. Bove[1*], P. Brotto[1], G. Calzolai[3], F. Cassola[1], F. Cavalli[2], P. Fermo[4], J. Hjorth[2], D. Massabò[1], S. Nava[3], A. Piazzalunga[5], C. Schembari[2], P. Prati[1]

[1] Department of Physics, University of Genoa, and INFN, 16146, Genoa, Italy
[2] European Commission, Joint Research Centre (JRC), Institute for Environment and Sustainability (IES), Air and Climate Unit, I - 21027 Ispra (VA), Italy
[3] Department of Physics and Astronomy, University of Florence, and INFN, 50019, Sesto Fiorentino (FI), Italy
[4]Department of Chemistry, University of Milan, Milan, 20133, Italy
[5] Department of Earth and Environmental Sciences, University of Milano Bicocca, 20126, Milan, Italy

*corresponding author e-mail address: mcbove@ge.infn.it +390103536325

Abstract

A PM10 sampling campaign was carried out on board the cruise ship Costa Concordia during three weeks in summer 2011. The ship route was Civitavecchia-Savona-Barcelona-Palma de Mallorca-Malta (Valletta)-Palermo-Civitavecchia. The PM10 composition was measured and utilized to identify and characterize the main PM10 sources along the ship route through receptor modelling, making use of the Positive Matrix Factorization (PMF) algorithm. A particular attention was given to the emissions related to heavy fuel oil combustion by ships, which is known to be also an important source of secondary sulphate aerosol. Five aerosol sources were resolved by the PMF analysis. The primary contribution of ship emissions to PM10 turned out to be (12 ± 4)%, while secondary ammonium sulphate contributed by (35 ± 5)%. Approximately, 60% of the total sulphate was identified as secondary aerosol while about 20% was attributed to heavy oil combustion in ship engines. The measured concentrations of methanesulphonic acid (MSA) indicated a relevant contribution to the observed sulphate loading by biogenic sulphate, formed by the atmospheric oxidation of dimethyl sulphide (DMS) emitted by marine phytoplankton.

Keywords: PM10, ship emissions, Mediterranean Basin, source apportionment

1. Introduction

The contribution of diverse anthropogenic and natural emissions sources, such as highly populated and industrial coastal areas, intense ship traffic, forest fire emissions and Sahara dust outbreaks, together with meteorological and geographical peculiarities, make the Mediterranean Basin one of the most polluted regions on Earth in terms of ozone concentrations and aerosol loading (Lelieveld et al, 2002, Velchev et al, 2011). This is caused by local emissions as well as transport of air pollution from outside the Mediterranean region. Ship emissions are an important source of pollution in this region and represent significant and growing contributors to air quality degradation in coastal areas (Van Aardenne et al., 2013). Emissions of exhaust gases and particles from the oceangoing ships affect the chemical composition of the atmosphere, climate and regional air quality (Eyring et al., 2005). In recent years, particle emissions from ships and harbour activities became a concern for air quality and object of several scientific investigations (Moreno et al., 2010, Becagli et al., 2012, Cesari et al., 2014, Bove et al., 2014). A number of studies have shown that ship exhaust particles contain V and Ni and these elements have been used as markers to investigate primary ship emissions using receptor models (Mazzei et al., 2008, Viana et al., 2009; Cuccia et al., 2010, Pandolfi et al., 2011, Salameh et al., 2015). The Joint Research Centre of the European Commission (JRC, EC) has carried out an air quality monitoring program from 2006 to 2014, based on observations from a cruise ship following a regular route in the Western Mediterranean. In the framework of a collaboration agreement between the JRC and Costa Crociere, continuous measurements of atmospheric pollutants were carried out on cruise ships from spring to autumn. During two campaigns in particular, in 2009 and 2010, a two-stage streaker sampler (Formenti et al., 1996) was installed on the ship. The elemental composition of the fine and coarse fraction of PM10, separately collected by the streaker on an hourly basis, was measured by PIXE analysis (Schembari et al., 2014). These datasets were used for an investigation of the influence of ship emissions on the composition of aerosols over the sea through a source apportionment analysis by PMF as well as by chemical marker compounds. The ship emissions were found to be an important source of aerosols in the Western Mediterranean, however a quantification of their impacts by PMF was not obtained. That experiment did not disentangle primary and secondary sources of sulphate and did not resolve the contribution of primary aerosol from ships, presumably because of the insufficient chemical speciation of PM10. A mixed combustion source, which showed evidence of a direct

connection with ship emissions was found to contribute by 55%, 63% and 80% to PM10, Black Carbon and sulphate, respectively (Schembari et al., 2014). In summary, the results of the previous campaigns indicated a significant impact of ship emissions to PM levels in the explored area but were not conclusive. In this context, a new PM10 sampling campaign was organized in the summer of 2011, to complete the information of the previous studies and to get a better description of PM sources. An extensive characterisation of PM10 samples, collected using a sequential filter sampler, was addressed; the obtained data were analysed by PMF and used to identify and characterize the main PM10 sources met along the route.

2. Material and methods

2.1 Monitoring campaign

The monitoring station was placed in a cabin at the front of the top deck of the ship "Costa Concordia". It permitted to perform continuous measurements of NO_X, SO_2, O_3 and Black Carbon (BC), the last one by means of an Aethalometer (AE 21, 2 wavelengths, Magee Scientific, USA) (Schembari et al., 2014). The aerosol sampling campaigns were carried out during three weeks of summer 2011: July 18-25, August 15-22 and September 12-19. PM10 samples were collected on Quartz filters (47mm diameter, flow rate 2.3 m^3 h^{-1}) using a Sven Leckel Ingenieurburo sequential sampler, placed on the top of the cabin where the monitoring and meteorological station were also located. The sampling was carried out on a variable time basis: the sampler was started 1 h after the departure from each harbour and stopped 1 h before the arrival in the next harbour. Each leg was then divided in periods of about 4-5 h with one filter sampled per each period. This resulted in a variable number of filters per open-sea leg and in a total number of about 20 filters per week.

2.2 Analytical methods

All filters were pre-conditioned for two days in a controlled room (temperature: 20±1˚C, relative humidity: 50±5%) before and after the sampling and then weighed using an analytical balance (sensitivity: 1 μg). Field blank filters were used to monitor possible artefacts. The compositional analyses were conducted using different methods. The elemental composition of filters sampled in August and September weeks, were measured by ED-XRF (Energy Dispersive - X Ray Fluorescence) using an ED-2000 spectrometer from Oxford Instruments (Ariola et al., 2006) for S, Cl, K, Ca, Ti, V, Cr, Mn, Fe, Ni, Cu, Zn, Br, Ba, Pb. For technical reasons, the concentrations of the same elements in the samples collected during

the July cruise were indeed determined by PIXE analysis at the HVEE 3 MV Tandetron accelerator, installed at the LABEC (LAboratorio BEni Culturali) laboratory of INFN in Florence (Calzolai et al., 2006; Lucarelli et al., 2013). The concentration values of S and K determined using ED-XRF were corrected for an average attenuation factor (Bove et al., 2014) to determine their mean values, whereas S, Cl, K resulted to be always below their Minimum Detection Limit when measured by PIXE. The Minimum Detection Limits obtained for both the techniques are shown in Table E1 in the electronic supplementary material. Finally, the analytical uncertainties are the sum of the systematic term on the calibration standards (5%) and of the statistical fluctuation on peak areas.

The water-soluble inorganic components of the PM10 were determined by Ion Chromatography (IC) using an ICS-1000 Ion Chromatography System (Dionex) at the University of Milan. In particular, for the extraction of the PM, a quarter of each filter was wetted previously and then three times with MilliQ water in an ultrasonic bath for 20 min (complete recovery, 98% ± 3%), renewing the water at each step (Piazzalunga et al., 2013). The extracts were analysed using IC to identify the major ionic species (i.e., Na^+, NH_4^+, K^+, Mg^{2+}, Ca^{2+},Cl^-, SO_4^{2-}, NO_3^-) with an overall 10% uncertainty for the ionic concentrations. The MSA (methanesulfonic acid) concentration values were also measured by IC with the same uncertainty. The lack of quantification of low-Z elements (due to the X-ray self-absorption and the high Si concentration in the quartz filters) was partially recovered by Ionic Chromatography analysis which was finally considered more accurate for such elements.

Information on meteorological parameters (wind speed and direction, temperature, humidity from the meteorological station of the ship) and on the ships position, speed and sailing direction, were also available (in 10 min intervals) and used to identify situations where the PM sampling might be influenced by the emissions of Costa Concordia itself. When the inlets of the measurement station were downwind the ship stack within an angle of ± 40˚, the data were discarded to avoid any risk of contamination.

Air mass back-trajectories were calculated using the US NOAA HYSPLIT model (http://ready.arl.noaa.gov/HYSPLIT.php) with GDAS meteorological data. For each filter, five-day back trajectories arriving at 50 m and 500 m above sea level were calculated for the positions where the filter sampling ended, to evaluate the different air masses arriving over the sea in the three cruise weeks. During summer 2011, the route of the ship was Civitavecchia-Savona-Barcelona-Palma de Mallorca-Malta (Valletta)-Palermo-Civitavecchia (see Figure E1 in the electronic supplementary material).

2.3 Aerosol composition: mass closure

Details on the method to obtain the aerosol composition is described in Schembari et al. (2014). Briefly, concentration values of SO_4^{2-}, NH_4^+ and NO_3^- were directly retrieved from the IC analysis, while sea salt and dust were obtained from raw data and conversion factors: sea salt was calculated from Na^+ and Cl^- concentration values, taking into account the seawater composition (Seinfeld and Pandis, 1998); dust was obtained by multiplication of non-sea-salt calcium $nssCa^{2+}$ (calculated by subtracting from total measured Ca^{2+}, the fraction in sea salt given by multiplication of Na^+ by Ca^{2+}:Na^+ ratio in seawater composition, Seinfeld and Pandis, 1998) by 5.6 (the value retrieved by Putaud et al. (2004) for a background site, would vary for any other kind of station).

2.4 Receptor model-PMF

Positive Matrix Factorization (PMF) was used to identify and characterize the major PM10 sources along the ship route. PMF has been described in detail by its developers (Paatero and Tapper, 1994), it has been adopted in several studies for PM receptor modelling and has rapidly become a reference tool in this research field (e.g., Qin et al., 2006; Escrig et al., 2009; Contini et al., 2012; Cuccia et al., 2013). In this work, the PMF2 program (Paatero, 2010) and the methodology described in Bove et al. (2014) was used. The PMF analyses were carried out using the data collected from the three weeks of the summer 2011. The variables were selected according to the signal-to-noise criterion (Paatero and Hopke, 2003) and 14 series of concentration values were finally retained for the PMF study: Ti, V, Fe, Ni, MSA, Cl^-, NO_3^-, SO_4^{2-}, Na^+, NH_4^+, K^+, Mg^{2+}, Ca^{2+}, BC. The Polissar et al. (1998) procedure was used to assign concentration data and their associated uncertainties; the Cl^-, NO_3^-, Na^+, Mg^{2+} uncertainties only were increased of 20% in the PMF runs for down weighting these elements which resulted ubiquitous among the factors. The number of samples considered in the PMF run (55) satisfies the criteria set in Thurston and Spengler, (1985). PMF results are affected by the rotational ambiguity (Paatero et al., 2002) and rotations are directly implemented in the minimisation algorithm using the FPEAK parameter (Paatero, 1997). In the analysis, the parameters obtained from the scaled residual matrix, IM (the maximum individual column mean), and IS (the maximum individual column standard deviation), together with Q-values (goodness of fit parameter) were examined to find the most reasonable solution. The best rotation for each factor was chosen in the FPEAK range from -2 to +2 by discarding the solutions corresponding to profiles without physical meaning (i.e., the sum of elemental concentrations exceeded 100%) and selecting those generating concentration ratios between

the tracer elements of the natural sources (e.g., sea salt, crustal matter) comparable to literature values (Bove et al., 2014).

3. Results and discussion

3.1 Meteorological conditions

The sea level pressure composite mean and anomalies over the Mediterranean basin during the three campaigns according to the NCEP/NCAR Reanalysis (Kalnay et al. 1996), are shown in Figure E2 in the electronic supplementary material. While in August and in September the synoptic conditions were characterized by the expansion towards the Mediterranean of the Azores Anticyclone, in line with seasonal climatology (especially in August, whereas a slightly negative anomaly is found in September), in July the situation was very peculiar. In this case, the anticyclonic system is confined over the Atlantic, favouring the development of low-pressure systems across Central Europe and the Mediterranean Basin, where a strong negative pressure anomaly can be seen.

The meteorological parameters recorded during the three cruises by the on-board instrumentation are reported in Figure E3 in the electronic supplementary material and confirm what is suggested by the synoptic analysis. In particular, pressure exhibited lower average values and larger variability in July, associated to episodes of strong wind and, as a consequence, rough sea along the route. On the contrary, during the two campaigns in August and September, more stable conditions were encountered, with higher pressure values and generally lighter winds, apart from the last leg of the September cruise, when the passage of an Atlantic frontal system determined a sudden pressure drop and wind speed increase.

The meteorological conditions along the ship route during the most relevant strong wind episodes were also assessed using a 32-year hindcast, recently realized at the University of Genoa by means of simulations with the Weather Research and Forecasting (WRF, Skamarock et al. 2008) model on a domain covering the entire Mediterranean with a horizontal grid spacing of 10 km. Details about the modelling system are given in Mentaschi et al. (2015).

3.2 PM10 composition

The average PM10 concentration and its composition are reported in Table 1 whereas in Figure 1 the chemical composition as described in 2.3 Section for the three 2011 cruises, is shown. The $nssSO_4^{2-}$, NO_3^-, sea salt seem to be quite different between the July campaign and

the other two cruise weeks (Figure 1). Such a discrepancy is attributable to the peculiar meteorological conditions occurred in July, as discussed in the previous section. The balance between nitrate and ammonium sulphate also shows two different well defined situations. During July and for some samples collected in September, ammonium and nitrate ions exactly balance, this highlighting the lack of ammonium sulphate. On the contrary, in August the sum of nitrate and sulphate ions are completely balanced by ammonium (Figure 2a). Furthermore, the ratio $(SO_4^{2-} + NO_3^-):NH_4^+$ shows increases correlated with Cl^- concentration values (Figure 2b). Figure 3 shows the anti-correlation between chlorine and sulphate concentration values: all these pieces of information point at the presence of air masses of two different origin which affect our samples as also indicated by back trajectory analysis. The air masses reaching the ship route in July, had been mainly over the sea for at least the previous 24 h; during the August and September cruises, the impacting air masses passed mostly over the continental areas, suggesting a larger contribution from the transport of terrestrial pollutants to the open sea. An example is shown in Figure E4 of the electronic supplementary material. In conclusion, when the air masses reached the ship coming from the continent, sulphate concentrations increased and the ratio $(SO_4^{2-} + NO_3^-) :NH_4^+$ approached 1. On the contrary, sulphate concentration values remained low without any sizeable presence of ammonium sulphate when the aerosol impacting the ship was mainly of marine origin.

The primary contribution of ship emissions to PM10 can be calculated on the basis of previous research works (Agrawal et al., 2009; Zhao et al., 2013) and using the equation:

$$PM_a = R\frac{V_a}{F_{V,HFO}} \quad (1)$$

R = 8205.8 is the average ratio of PM2.5 to normalized V emitted (ppm) suggested in Agrawal et al. (2009), which could be universally applied to other locations with HFO burning ship emissions; V_a is the ambient concentration of V (ng m^{-3}), whilst $F_{V, HFO}$ is a term indicating the typical V content (in ppm) in HFOs used by vessels. We used the same average value of $F_{V, HFO}$ = (65 ± 25) ppm, in agreement with Cesari et al., (2014). According to eq. (1), the primary PM10 from ship traffic ranged from 0.7 to 3.4 μg m^{-3}; similar values had been previously obtained in some port sites (Viana et al., 2009).

3.3 Sulphate apportionment

The contributions of different sources to the sulphate concentration was evaluated on the basis of specific markers as described in Table E2 in the electronic supplementary material. The main components of the sulphate are the sea salt sulphate ($ssSO_4^{2-}$), that is the amount of sulphate present in sea salt particles, and non-sea-salt sulphate. The non-sea-salt sulphate ($nssSO_4^{2-}$) is defined as the amount of the sulphate present in particles in excess of what expected from sea salt particles, and has three contributions: anthropogenic, biogenic and crustal $nssSO_4^{2-}$. According to some literature works, methanesulfonic acid can be used as a marker for quantifying the biogenic non-sea salt sulphate ($nssSO_4^{2-}{}_{bio}$). The ratio between MSA and $nssSO_4^{2-}{}_{bio}$ depends on the season (Kouvarakis et al., 2002), latitude (Chen et al., 2012) and temperature (Bates et al. 1992). In a previous work (Schembari et al., 2014), the $nssSO_4^{2-}{}_{bio}$ was estimated starting from the measurement of MSA concentration in the samples through the relation by Bates et al. (1992) even if that equation was obtained during of field campaign in the eastern Pacific Ocean.

In our data set we identified a sample marked in Figure 3, that seems to be affected by a strong presence of fresh marine aerosols: the ratio Cl^-:Na^+ = 1.094 and Mg^+:Na^+= 0.24 are very similar to those reported in literature for the fresh marine aerosol, respectively 1.17, and 0.25 (Keene et al., 1986). Furthermore, the ionic balance is fully respected: 162 neq m^{-3} of anions vs. 160 neq m^{-3} of cations and the sulphate is not fully balanced from ammonium, this highlighting the presence of a sulphates source different from the anthropogenic ones. With this sample, the direct calculation (details are shown in Table E2b in the electronic supplementary material) of the $nssSO_4^{2-}{}_{bio}$ concentration using the diagnostic ratios reported in literature work (Keene et al., 1986), is possible and the MSA:$nssSO_4^{2-}{}_{bio}$ ratio was found to be 0.08 against the value of 0.03 which would result from the Bates's formula. Finally, we adopted MSA:$nssSO_4^{2-}{}_{bio}$ = 0.08 for the whole campaign and to derive the sulphate apportionment.

The results of such calculations for the three cruises are reported in Table 2 and Figure 8. Large concentration values of $nssSO_4^{2-}$ were obtained for all the three weeks, while highest values of $ssSO_4^{2-}$ and lowest values of $nssSO_4^{2-}$ were observed in July (Figure 1). The latter were in coincidence with a quite high wind speed, in particular during the Savona-Barcelona and Palermo-Civitavecchia legs. The analysis of wind speed and direction, both measured on board and obtained by hindcast simulations with the WRF-ARW model (see also Figure E5 and E6 in the electronic supplementary material), highlighted that it blew from the sea and its velocity increased rapidly during the last part of the routes, close to the Barcelona coast and to Civitavecchia, respectively. This observation confirms the sea salt dependence on the local

wind speed in the Mediterranean Basin (Bergametti et al. (1989a) Chabas and Lefèvre (2000); Contini et al., 2010). The main contribution to $nssSO_4^{2-}$ was of anthropic origin in August and September, whereas in July $nssSO_4^{2-}{}_{bio}$ was prevailing, probably due to the particular meteorological conditions that determined high sea salt concentrations. The $nssSO_4^{2-}{}_{anthr}$ contributed to PM10 by 5%, 25% and 18%, in July, August and September, respectively, while the $nssSO_4^{2-}{}_{bio}$ was on average 9%, 5% and 3% of PM10 in the same periods. The $nssSO_4^{2-}{}_{crust}$, as estimated by this approach, remained always around 1% of PM10.

The above-discussed results can be compared with those collected in the similar cruise in June 2010 (Schembari et al., 2014), also reported in Table 2. The previous sulphate apportionment showed similar contributions to 2011 data for $nssSO_4^{2-}{}_{crust}$ and $ssSO_4^{2-}$. Indeed, the meteorological conditions in June 2010 were quite resembling those found in July 2011, with cool temperatures and intense winds (see Schembari et al. 2014). The $nssSO_4^{2-}{}_{bio}$ showed higher average contributions if compared to values obtained in the three 2011 cruises. Higher values of $nssSO_4^{2-}{}_{anth}$ were also obtained in 2010 with respect to the 2011 campaigns, with the only exception of the August cruise, when higher levels of $nssSO_4^{2-}{}_{anth}$ were found.

3.4 PMF results

The database used as input to PMF included data obtained by the analysis of filters sampled along open-sea legs while samples collected when the ship was manoeuvring or hotelling in the harbours and when the sampling station was downwind the ship stack, were excluded. The database was completed with the time series of hourly BC concentration values and PM10 mass concentration.

Five factors were resolved and identified by PMF for PM10 obtaining the best solution with FPEAK =0: *Secondary Sulphate, Reacted dust, Biomass burning, Sea salt* and *Heavy oil combustion.* Source profiles and explained variations (EV) parameters are shown in Figure 4, while the average PM10 apportionment is given in Figure 5.

PMF-Factor 1 was identified as the contribution due to *Secondary Sulphate* looking at the high EVs for SO_4^{2-} and NH_4^+ and the relevance of these compounds in the chemical profile (Figure 4). The average concentration ratio for SO_4^{2-}:NH_4^+ in the factor is 2.1 ± 0.1, which is slightly lower than the stoichiometric figure for ammonium sulphate (i.e. SO_4^{2-}:NH_4^+= 2.7). The average relative contribution of this factor to the PM10 mass is (35 ± 5)%, with highest concentrations observed during August and lowest in July as reported in Table 3. The PMF result is comparable, within its uncertainty, with the direct calculation of the average abundance of ammonium non-sea-salt sulphate in PM10 of (39 ± 4)%, discussed in Section

3.2. The quite low concentration value of July reported in Figure 6 confirms the observations obtained by the measurements.

PMF-Factor 2 was characterised by high EV values for Ti and Fe, this suggesting a contribution by mineral dust, and by a relevant fraction of SO_4^{2-}, NO_3^-, NH_4^+ and BC in the source profile (Figure 4). The mineral particles aged in the atmosphere and then changed their original composition, getting mixed/coated with organic and inorganic ions (sulphate and nitrate) and BC (Fairlie et al., 2010). For this reason, this factor was labelled as *Reacted dust,* also in agreement with other source profiles obtained by PMF in Mediterranean sites (Perrone et al., 2013, Cesari et al., 2014). The temporal pattern of this factor showed highest concentrations along the Barcelona-Palma legs (see also Figure 6), in particular near the Palma coast. Moreover, this source profile is quite similar to the mineral dust profile obtained by PMF analysis of the data sampled in a site located at Palma de Mallorca (Pey et al., 2013), which includes anthropogenic dust emissions from the harbour too. For this reason, the fraction of PM10 attributed by PMF to *Reacted dust,* even if it appears consistent with the "chemical" apportionment described in Section 2.3, is not comparable to the pure dust composition.

PMF-Factor 3 was assigned to *Biomass burning* because it was characterized by high contributions of BC, SO_4^{2-}, NH_4^+ and K^+ in the source profile (Figure 4) and by high EV values for BC and K^+ in agreement with other works which adopted K^+ as tracer of biomass burning (Belis et al., 2011). High concentration values were detected along the Malta-Palermo leg, both in August and September (see also Figure 6). Maximum values were observed with high wind speed and prevailing direction from the Sicilian coast and from the city of Palermo. The contribution of the source, on average (27 ± 5)% of PM10, seems to be excessive considering the summer period in which the measurements were performed. Actually, this is not a pure profile because includes the mixing with other sources like re-suspended dust coming from the continents nearby. This aspect is confirmed also by the presence of Ca^{2+} element, which instead is absent in the "Reacted dust" profile.

PMF-Factor 4 was identified as *Sea salt* since it was characterized by high EV values for NO_3^-, Cl^-, Na^+, Mg^{2+} and MSA (Figure 4). The Cl^-:Na^+ ratio in the profile is equal to 0.2, which is much smaller than both the 0.9 mean ratio obtained in the 2009 and 2010 cruises (Schembari et al ., 2014) and the 1.17 ratio of fresh sea salt particles (Keene et al., 1986). This can be due to evaporation of HCl to the atmosphere which occurs in marine air samples (Perrone et al., 2013, Cuccia et al., 2013). The PMF algorithm could not distinguish fresh and aged sea salt: in the *Sea salt* source profile (Figure 4), the presence of the secondary nitrates

and MSA^- due to the oxidation of dimethyl sulphide emitted from the sea suggested the mixing with secondary components of PM10. The average fraction of PM10 attributed to this factor was (19 ± 4)%, in agreement with the (27 ± 5)% value obtained as the sum of Sea salt and Nitrates components obtained evaluated by chemical analysis (Section 2.3). The sea salt concentration was higher in July than in August and September as highlighted in Table 3: this confirms the occurrence of sea salt events during the Savona-Barcelona and Palermo-Civitavecchia legs as described in Section 3.2.

PMF-Factor 5 was finally identified as *Heavy oil combustion* because it was characterized by high EV values for V and Ni, typical tracers of heavy oil combustion (Mazzei et al., 2008, Viana et al., 2009). The V:Ni concentration ratio in the source profile is 2.6 ± 0.1, in agreement with the 2.9 ± 0.4 value obtained by PMF during the previous campaigns (Schembari et al., 2014) and with the conclusions of several other literature works which recognized such value as typical of ship emissions (Agrawal et al., 2008, Mazzei et al., 2008, Cuccia et al., 2010, Pandolfi et al., 2011, Bove et al., 2014). The source profile was enriched in sulphate with SO_4^{2-}:V = 67 ± 4. The initial SO_4^{2-}:V ratio in the particulate exhaust (PM2.5) of the main engine of different oceangoing container vessels is reported to be in the range 11–27 (Agrawal et al., 2008). However, the amount of SO_4^{2-} in the air mass is expected to grow fast due to SO_2 conversion into sulphate; this conversion is faster in high UV radiation and high humidity conditions (Restad et al., 1998, Becagli et al., 2012). Actually, the measured SO_4^{2-}:V ratio (similar to the SO_4^{2-}:V ratio in the profile) is lower in July than the other two cruise weeks, confirming the higher influence of marine air masses as observed in Section 3.2 and, therefore, of the ship emissions along the route. Ship emissions contributed on average to (12 ± 4)% of PM10. This figure is in agreement with the (16 ± 11)% percentage evaluated considering the measured V as a marker for the combustion in ship engines (3.2 Section).

The apportionment of single PM10 species is given in Figure 7. Notably, NO_3^- was mainly associated with *Sea salt* (on average 95%) supporting the nature of aged marine source (Cuccia et al., 2013), whereas NH_4^+ was primarily associated with one of the secondary components of PM10, i.e. *Secondary Sulphate* (on average: 80%). On average, (23 ± 9)% of the SO_4^{2-} was attributed to *Heavy oil combustion*. The Sulphate apportionment resolved by PMF appears to be different in the three cruises (see also Figure 8). The apportionment seems to be quite similar in August and September while an increase of the total SO_4^{2-} attributed to *Heavy oil combustion* in association with the Sea salt events (3.3 Section) was observed in July. The latter can be explained by the possible contamination in the *Heavy oil combustion*

profile of the biogenic fraction of the sulphates (the measured biogenic sulphate was much larger than the anthropogenic one in July); this is probably due to the influence of meteorological conditions and air masses which remained over the sea for several hours, producing the association of both sources. Moreover, the average measured MSA: $nssSO_4^{2-}$ ratio for the three cruise weeks is the same value found in the *Heavy oil combustion* factor obtained by PMF analysis to support the biogenic contamination of the sulphate in the profile.

3.3.1 Sources comparison

The new study provided more complete and clear information than the analysis performed in the past years (Schembari et al., 2014). Due to the lack of a complete chemical speciation, only four sources were resolved in 2010 and in particular the PMF did not resolve secondary and primary sources of sulphate. A *Combustion* source only, which showed evidence of a contribution by ship emissions, was found to contribute by (55 ± 4)% to PM10. The main scope of the 2011 experiment was to separately quantify the contribution of ship emissions and of secondary sulphate to PM10. This objective was achieved: in 2011 the *Secondary Sulphate* and *Heavy oil combustion* were found to account for (35 ± 5)% and (12 ± 4)% of PM10, respectively. The *Combustion* factor identified in the previous campaigns is comparable with the sum of *Secondary Sulphate* and *Heavy oil combustion* sources in 2011. Moreover, the source *Not identified* by PMF in 2009-2010 was recognized as *Biomass burning* with the 2011 dataset since it is characterized and traced by high contributions of BC and K^+. For *Sea salt* and *Reacted dust* a similar mean contribution to PM10 was obtained in 2010 and 2011.

The names given to the sources of the five PMF factors obviously represent a simplification; it is clear that there must be several additional minor sources that have contributed to the observed aerosol composition; in particular, land-based traffic and industrial sources. Thus, the five source profiles are not representing 'pure' sources and the names given to them will only reflect what is believed to be the principal source contributing to this profile.

4. Conclusions

PM10 aerosol samples collected during three campaigns on board a cruise ship from July to September 2011 were analysed to determine their chemical composition and to improve the source apportionment obtained during previous studies performed on board

cruise ships in the Western Mediterranean. The biogenic fraction of the sulphate was prevailing during the July campaign, together with a higher contribution of the ship emissions, probably due to the influence of predominantly marine air masses along the ship route. Five sources were resolved and identified by PMF analysis with the new data sets: *Secondary Sulphate, Reacted dust, Biomass burning, Sea salt* and *Heavy oil combustion*. Heavy oil combustion by ship engines was identified using V and Ni as tracers. Secondary ammonium sulphate was found to be an important source of aerosol in Western Mediterranean. The experiment allowed the identification of a contribution of primary ship emissions to PM10. This contribution turned out to be (12 ± 4)%, while secondary ammonium sulphate contributed by (35 ± 5)%. Approximately 60% of the total sulphate was attributed to secondary sources and around 20% was attributed to *Heavy oil combustion* considering the measuring campaigns not influenced by strong sea salt events.

Acknowledgements

Thanks are due to Costa Crociere and to the technical assistance of V. Ariola from the Department of Physics of the University of Genoa. This work has been partially supported by INFN under the grant for the MANIA experiment.

References

Agrawal, H., Welch, W.A., Miller, J.W., Cocker, D.R., 2008. Emission measurements from a crude oil tanker at sea. Environmental Science Technology 42, 7098-7103.

Agrawal, H., Eden, R., Zhang, X., Fine, P.M., Katzenstein, A., Miller, J.W., Ospital J., Teffera S., Cocker D.R., 2009. Primary particulate matter from ocean-going engine in the southern California air basin. Environmental Science Technology 43, 398–402.

Ariola, V., D'Alessandro, A., Lucarelli, F., Marcazzan, G., Mazzei, F., Nava, S., Garcia Orellana, I., Prati, P., Valli, G., Vecchi, R., Zucchiatti, A. 2006. Elemental characterization of PM10, PM2.5 and PM1 in the town of Genoa (Italy). Chemosphere 62, 226-232.

Bates, T., Calhoun, J., Wang, Y., Quinn, P., 1992. Variations in the methanesulphonate to sulphate molar ratio in submicrometer marine aerosol particles over the south pacific ocean. Journal of Geophysical research 97, 9859-9865.

Becagli, S, Sferlazzo, D.M., Pace, G., Di Sarra, A., Bommarito, C., Calzolai, G., Ghedini, C., Lucarelli, F., Meloni, D., Monteleone, F., Severi, M., Traversi, R. and Udisti R., 2012. Evidence for heavy fuel oil combustion aerosols from chemical analyses at the island of Lampedusa: a possible large role of ships emissions in the Mediterranean. Atmospheric Chemistry and Physics 12, 3479–92.

Belis, C.A., Cancelinha, J., Duane, M., Forcina V, Pedroni V, Passarella R, Tanet, G., Douglas, K., Piazzalunga, A., Bolzacchini, E., Sangiorgi, G.M.L., Perrone, M.G., Ferrero, L., Fermo, P., Larsen, B.R., 2011. Sources for PM air pollution in the Po Plain, Italy: I. Critical comparison of methods for estimating biomass burning contributions to benzo(a)pyrene. Atmospheric Environment 45, 7266–75.

Belis C.A., Karagulian, F., Larsen, B.R., Hopke, P.K, 2013. Critical review and meta-analysis of ambient particulate matter source apportionment using receptor models in Europe. Atmospheric Environment 69, 94-108.

Bergametti, G., Dutot, A.-L., Buat-Menard, P., Losno, R., and Remoudaki, E., 1989a. Seasonal variability of the elemental composition of atmospheric aerosol particles over the north western Mediterranean, Tellus 41B, 353–361.

Birch, M. E., Cary, R. A., 1996. Elemental carbon-based method for monitoring occupational exposures to particulate diesel exhaust. Aerosol Science and Technology 25, 221-241.

Bove, M.C., Brotto, P., Cassola, F., Cuccia, E., Massabò, D., Mazzino, A., Piazzalunga, A., Prati, P., 2014. An integrated PM2.5 source apportionment study: Positive Matrix Factorisation vs. the Chemical Transport Model CAMx. Atmospheric Environment 94, 274-286.

Calzolai, G., Chiari, M., García Orellana, I., Lucarelli, F., Migliori, A., Nava, S., Taccetti, F., 2006. The new external beam facility for environmental studies at the Tandetron accelerator of LABEC. Nuclear Instrument Methods B249 (1-2), 928-931.

476 Cavalli, F., Putaud, J.P., Viana, M., Yttri, K.E., Gemberg, J., 2010. Toward a standardised
477 thermal-optical protocol for measuring atmospheric organic and elemental carbon: the
478 EUSAAR protocol. Atmospheric Measurement Techniques 3, 79-89.
479
480 Cesari, D., Genga, A., Ielpo, P., Siciliano, M., Mascolo, G., Grasso, F.M., Contini, D., 2014.
481 Source apportionment of PM2.5 in the harbour–industrial area of Brindisi (Italy):
482 Identification and estimation of the contribution of in-port ship emissions. Science of the
483 Total Environment 497–498, 392–400.
484
485 Chabas, A. and Lefèvre, R. A., 2000. Chemistry and microscopy of atmospheric particulates
486 at Delos (Cyclades-Greece). Atmospheric Environment 34, 225–238.
487
488 Chen, L. Wang, J., Gao, Y., Xu, G., Yang, X., Lin, Q., Zhang, Y., 2012. Latitudinal
489 distributions of atmospheric MSA and MSA/nss-SO_4^{2-} ratios in summer over the high latitude
490 regions of the Southern and Northern Hemispheres. Journal of geophysical research 117,
491 D10306, doi:10.1029/2011JD016559.
492
493 Chiari, M., Lucarelli, F., Mazzei, F., Nava, S., Paperetti, L., Prati, P., Valli, G., Vecchi, R.
494 2005. Characterization of airborne particulate matter in an industrial district near Florence by
495 PIXE and PESA. X-Ray Spectrometry 34, 323-329.
496
497 Chow, J.C., Watson, J.G., 1999. Ion chromatography in elemental analysis of airborne
498 particles. In: Landsberger, S., Creatchman, M. (Eds.), Elemental Analysis of Airborne
499 Particles, vol. 1. Gordon and Breach Science, Amsterdam, 97-137.
500
501 Contini, D., Genga, A., Cesari, D., Siciliano, M., Donateo, A., Bove, M.C., Guascito, M.R.,
502 2010. Characterisation and source apportionment of PM10 in an urban background site in
503 Lecce. Atmospheric Research 95 (1), 40-54.
504
505 Contini, D., Belosi, F., Gambaro, A., Cesari, D., Stortini, A., Bove, M.C., 2012. Comparison
506 of PM10 concentrations and metal content in three different sites of the Venice Lagoon: an
507 analysis of possible aerosol sources. Journal of Environmental Science 24 (11), 1954-1965.
508

509 Cuccia, E., Bernardoni, V., Massabò, D., Prati, P., Valli, G., Vecchi, R., 2010. An alternative
510 way to determine the size distribution of airborne particulate matter. Atmospheric
511 Environment 44, 3304-3313.
512
513 Cuccia, E., Massabò, D., Ariola, Bove, M.C., Fermo, P., Piazzalunga, A., Prati, P., 2013. Size
514 resolved comprehensive characterization of airborne particulate matter. Atmospheric
515 Environment 67, 14-26.
516
517 Eyring, V., Köhler, H.W., Van Aardenne, J., Lauer, A., 2005. Emissions from international
518 shipping: 1. The last 50 years. Journal of Geophysical Research Atmosphere 110, D17305.
519
520 Escrig, A., Monfort, E., Celades, I., Querol, X., Amato, F., Mingiullon, M.C., Hopke, P.K.,
521 2009. Application of optimally scaled target factor analysis for assessing source contribution
522 of ambient PM10. Journal of Air Waste Management Association 59, 1296-1307.
523
524 Fairlie, T.D., Jacob, D.J., Dibb, J.E., Alexander, B., Avery, M.A., Van Donkelaar, A., Zhang,
525 L., 2010. Impact of mineral dust on nitrate, sulphate, and ozone in transpacific Asian pollution
526 plumes. Atmospheric Chemistry and Physics 10, 3999-4012.
527
528 Formenti, P., Prati, P., Zucchiatti, A., Lucarelli, F., Mandò, P.A., 1996. Aerosol study in the
529 Genova area via a two stage streaker and PIXE analysis. Nuclear Instrument Methods B113,
530 359-362.
531
532 Kalnay, E., Kanamitsu, M., Kistler, R., Collins, W., Deaven, D., Gandin, L., Iredell, M., Saha,
533 S., White, G., Woollen, J., Zhu, Y., Leetmaa, A., Reynolds, R., Chelliah, M., Ebisuzaki, W.,
534 Higgins, W., Janowiak, J., Mo, K. C., Ropelewski, C., Wang, J., Jenne, R., Joseph, D., 1996.
535 The NCEP/NCAR 40-Year Reanalysis Project, Bulletin of the American Meteorological
536 Society 77, 437-471.
537
538 Keene, W. C., Pszenny, A. A. P., Galloway, J. N. Hawley M. E., 1986. Sea-Salt Corrections
539 and Interpretation of Constituent Ratios in Marine Precipitation. Journal of Geophysical
540 research 91, 6647-6658.
541

Kouvarakis, G. and Mihalopoulos, N., 2002. Seasonal variation of dimethylsulfide in the gas phase and of methanesulfonate and non-sea-salt sulphate in the aerosols phase in the Eastern Mediterranean atmosphere. Atmospheric Environment 36, 929–938.

Lelieveld, J., Berresheim, H., Borrmann, S., Crutzen, P.J., Dentener, F., 2002. Global air pollution crossroads over the Mediterranean. Science 298, 794-799.

Lucarelli, F., Calzolai, G., Chiari, M., Giannoni, M., Mochi, D., Nava, S., Carraresi, L., 2013. The upgraded external-beam PIXE/PIGE set-up at LABEC for very fast measurements on aerosol samples. Nuclear Instruments and Methods in Physics Research. http:// dx.doi.org/10.1016/j.nimb.2013.05.099.

Mazzei, F., D'Alessandro, A., Lucarelli, F., Nava, S., Prati, P., Valli, G., Vecchi, R., 2008. Characterization of particulate matter sources in an urban environment. Science of Total Environment 401, 81-89.

Mentaschi, L., Besio, G., Cassola, F., Mazzino, A., 2015. Performance evaluation of WavewatchIII in the Mediterranean Sea. Ocean Modelling 90, 82-94.

Moreno, T., Perez, N., Querol, X., Amato, F., Alastuey, A., Bhatia, R., Spiro, B., Hanvey, M., Gibbons, W., 2010. Physicochemical variations in atmospheric aerosols recorded at sea on board the Atlantic-Mediterranean 2008 Scholar Ship cruise (Part II): natural versus anthropogenic influences revealed by PM10 trace element geochemistry. Atmospheric Environment 44, 2563-2576.

Paatero, P., Tapper, U., 1994. Positive matrix factorization: a non-negative factor model with optimal utilization of error estimates of data values. Environmetrics 5, 111-126.

Paatero, P., 1997. Least squares formulation of robust, non-negative factor analysis. Chemometrics Intelligent Laboratory Systems 37, 23-35.

Paatero, P., Hopke, P.K., Song, X.H., Ramadan, Z., 2002. Understanding and controlling rotations in factor analytic models. Chemometrics and Intelligent Laboratory Systems 60, 253-264.

576 Paatero, P., Hopke, P.K., 2003. Discarding or down weighting high-noise variables in factor
577 analytic models. Analytica Chimica Acta 490, 277-289.
578
579 Paatero, P., 2010. User's Guide for Positive Matrix Factorization Programs PMF2 and PMF3,
580 Part 1: Tutorial. University of Helsinki, Finland.
581
582 Perrone, M.R., Becagli, S., Garcia Orza, J.A., Vecchi, R., Dinoi A, Udisti, R., Cabello, M.,
583 2013. The impact of long-range-transport on PM1 and PM2.5 at a Central Mediterranean site.
584 Atmospheric Environment 71, 176-186.
585
586 Pey, J, Alastuey, A. Querol, X., 2013. PM10 and PM2.5 sources at an insular location in the
587 western Mediterranean by using source apportionment techniques. Science of the total
588 Environment 456-457, 267-277.
589
590 Piazzalunga, A., Bernardoni, V., Fermo, P., Vecchi, R., 2013. Optimisation of analytical
591 procedures for the quantification of ionic and carbonaceous fractions in the atmospheric
592 aerosol and applications to ambient samples. Analytical and Bioanalytical Chemistry 405,
593 1123-1132.
594
595 Polissar, A.V., Hopke, P.K., Paatero, P., Malm, W.C., Sisler, J.F., 1998. Atmospheric aerosol
596 nucleation and primary emission rates. Atmospheric Chemistry and Physics, 1339-1356.
597
598 Putaud, J.P., Van Dingenen, R., Dell'Acqua, A., Raes, F., Matta, E., Decesari, S., Facchini,
599 M.C., Fuzzi, S., 2004. Size-segregated aerosol mass closure and chemical composition in
600 Monte Cimone (I) during MINATROC. Atmospheric Chemistry and Physics 4, 889-902.
601
602 Qin, Y., Kim, E., Hopke, P.K., 2006. The concentration and sources of PM2.5 in metropolitan
603 New York City. Atmospheric Environment 40, 312-332.
604
605 Restad, K., Isaksen, I. S. A., and Berntsen, T. K., 1998. Global distribution of sulphate in the
606 troposphere: A three-dimensional model study. Atmospheric Environment 32, 3593–3609.
607
608 Salameh, D., Detournay A., Pey, J., Pérez, N., Liguori, F., Saraga D., Bove, M.C., Brotto P,
609 Cassola F., Massabò, D., Latella A., Pillon, S., Formenton, G., Patti, S., Armengaud, A., Piga,

610 D. Jaffrezoj, J.L. Bartzisf, J., Tolis, E., Prati, P. Querol, X., Worthama, H., Marchand, N.,
611 2015. PM2.5 chemical composition in five European Mediterranean cities: A 1-year study.
612 Atmospheric research 155, 102-117.
613
614 Schembari, C., Bove, M.C., Cuccia, E., Cavalli, F., Hjorth, J., Massabò, D., Nava, S., Udisti,
615 R., Prati, P. 2014. Source apportionment of PM10 in the Western Mediterranean based on
616 observations from a cruise ship. Atmospheric Environment 98, 510-518.
617
618 Seinfeld, J.H., Pandis, S.N., 1998. Atmospheric Chemistry and Physics. John Wiley and Sons.
619
620 Skamarock, W.C., Klemp, J.B., Dudhia, J., Gill, D.O., Barker, D.M., Huang, X.Z., Wang, W.,
621 Powers, J.G., 2008. A Description of the Advanced Research WRF Version 3. Technical
622 report. Mesoscale and Microscale Meteorology Division, NCAR, Boulder, Colorado.
623
624 Thurston, G.D., Spengler, J.D., 1985. A quantitative assessment of source contributions to
625 inhalable particulate matter pollution in metropolitan Boston. Atmospheric Environment 19,
626 9-25.
627
628 Van Aardenne, J., A. Colette, B. Degraeuwe, P. Hammingh, M. Viana, I. de Vlieger, 2013.
629 The impact of international shipping on European air quality and climate forcing. EEA
630 Technical Report no. 4.
631
632 Vecchi, R., Valli, G., Fermo, P., D'alessandro, A., Piazzalunga, A., Bernardoni, V., 2009.
633 Organic and inorganic sampling artefacts assessment. Atmospheric Environment 43, 1713-
634 1720.
635
636 Velchev, K., Cavalli, F., Hjorth, J., Vignati, E., Dentener, F., Raes, F., 2011. Ozone over
637 Western Mediterranean Sea-results from two years of shipborne measurements. Atmospheric
638 Chemistry and Physics 11, 675-688.
639
640 Viana, M., Amato, F., Alastuey, A., Querol, X., 2009. Chemical Tracers of particulate
641 emissions from commercial shipping. Environmental Science Technology 43, 7472-7477.

642 Zhao, M., Zhang, Y., Maa, W., Fu, Q., Yang, X., Li, C., Zhou, B., Yu, Q., Chen., L., 2013.
643 Characteristics and ship traffic source identification of air pollutants in China's largest port.
644 Atmospheric Environment 64, 277–86.

FIGURE AND TABLE CAPTIONS

Figure 1. PM10 chemical composition obtained from raw data and conversion factors during July (top), August (centre) and September (bottom) campaigns. PM10 gravimetric values, which were affected by large uncertainties, are also shown in each panel as 1-sigma band delimited by the two dashed lines.

Figure 2. **a)** Ionic balance for the three cruise campaigns in neq m^{-3} **b)** the ratio between the sum of NO_3^- and SO_4^{2-} with NH_4^+ is compared with the Cl^- concentration.

Figure 3. Scatter plot between SO_4^{2-} and Cl^- concentrations. When the Cl^- concentrations are high (greater than 10 neq m^{-3}) the SO_4^{2-} concentrations are low. The marked data is the sample used to calculate the MSA/nss$SO_4^{2-}{}_{bio}$ ratio.

Figure 4. PMF profiles (left axis, coloured bars) and explained variation factors, EV (right axis, white circles) of the PM10 sources resolved in all the three cruise weeks in summer 2011.

Figure 5. Average source apportionment obtained by the PMF analysis of the PM10 data sets collected during the summer 2011.

Figure 6. Average apportionment of elements/compounds concentration obtained by PMF analysis calculated with the PM10 data sets of the whole field campaign.

Figure 7. Time trends of the five pollutant sources (factors) obtained by PMF analysis during the three cruise weeks in summer 2011.

Figure 8. Average apportionment of the total sulphate (relative values) obtained by PMF (right histograms) and by the chemical approach described in Section 3.3 (left histograms) for the three cruises of the 2011 campaign.

Table 1. Average PM10 composition and BC obtained by Aethalometer for the three campaigns in summer 2011: average (A) and standard deviation (St. Dev) of concentration values were calculated with the samples (reported as percentage frequency, F) with concentration values above their Minimum Detection Limit (MDL). For Cl, K and Ca both the total concentration by ED-XRF and the soluble fraction by IC are reported.

672 **Table 2**. Contributions to the total SO_4^{2-} concentration in absolute values, for the three cruise
673 weeks in 2011 and for the previous campaign in June 2010 determined with the method
674 described in Section 3.3.

675 **Table 3**. Average source apportionment obtained by the PMF analysis of the PM10 data sets
676 collected during the summer 2011 separately for the three cruise campaigns. The average
677 source apportionment is reported in absolute and relative values.

678

679 **Electronic supplement material**

680 **Figure E1.** Route of Costa Concordia during the three campaigns in summer 2011.

681 **Figure E2.** Sea level pressure composite mean (left) and anomalies (right) with respect to the
682 1981-2010 climatology for the July (top panel), August (center) and September (bottom)
683 campaigns, obtained from the NCEP/NCAR Reanalysis (images provided by the
684 NOAA/ESRL Physical Sciences Division, Boulder Colorado, from their web site at
685 http://www.esrl.noaa.gov/psd/).

686 **Figure E3**. Times series of temperature, relative humidity and pressure (top), and wind speed
687 (bottom) recorded by the meteorological instrumentation on board the ship during the three
688 campaigns.

689 **Figure E4**. Air mass back trajectories calculated using the HYSPLIT model, related to 21
690 July (right) and 16 August 2011 (left).

691 **Figure E5.** Time trends of sea salt component of PM10 obtained as described in Section 2.3
692 and correlation between wind velocity (km/h) (top figure) and wind prevalent direction
693 (bottom) along the open sea tracks considered.

694 **Figure E6.** 10-m wind fields simulated by the non-hydrostatic mesoscale model WRF-ARW
695 relative to the sea salt events: Savona-Barcelona tracks of the July 18 (top) and Palermo-
696 Civitavecchia tracks of the July 24 (bottom).

697 **Table E1**. Minimum detection limits for each species in ED-XRF and PIXE analysis; PIXE
698 analysis have been used for the samples relative to July week only.

699 **Table E2. a)** Relations used to calculate the different contributions to the total SO_4; sea salt
700 sulphate and not sea salt sulphate, divided in: anthropogenic, biogenic and crustal. A value of

701 0.498 was used for the ratio between SO_4 and Mg in seawater (Keene et al., 1986). Based on
702 the sulphur content in crustal material (Seinfield and Pendis, 1988), the ratio between SO_4 and
703 Ca in dust was estimated to be 0.097 g/g. Sea salt Ca was obtained as ssCa = 0.0437 *Na (
704 Keene et al., 1986) **b**) details of the calculation to extract the $nssSO_{4bio}$ concentration in a
705 sample influenced by fresh marine air (see text, Section 3.3).

ng m^{-3}			
	A	St. Dev	F
PM10	13113	4778	100%
S	1684	933	67%
Cl	209	376	38%
K	340	291	65%
Ca	151	120	93%
Ti	31	19	98%
V	16	13	95%
Cr	10	5	58%
Mn	5	4	75%
Fe	164	101	98%
Ni	7	5	87%
Cu	5	3	64%
Zn	16	15	87%
Br	7	5	58%
Ba	15	7	27%
Pb	4	3	16%
MSA	54	28	93%
Cl^-	381	452	98%
NO^{3-}	882	584	98%
SO_4^{2-}	3216	2254	100%
Na^+	1003	566	100%
NH_4^+	1043	869	100%
K^+	151	150	27%
Mg^{2+}	139	79	100%
Ca^{2+}	222	114	100%
BC	570	501	100%

ng m^{-3}	2010 June 7-14	2011 July 18-25	2011 August 15-22	2011 September 12-19
totSO_4^{2-}	4550	1760	4820	3100
ssSO_4^{2-}	280	420	150	250
nss$SO_4^{2-}_{crustal}$	30	30	60	40
nss$SO_4^{2-}_{biogenic}$	1290	870	750	400
nss$SO_4^{2-}_{anthropogenic}$	2950	440	3850	2410

Source	**July 18-25**		**August 15-22**		**September 12-19**	
	(ng m^{-3})	(%)	(ng m^{-3})	(%)	(ng m^{-3})	(%)
Secondary Sulphate	730 ± 170	14 ± 3	5730 ± 720	41 ± 5	3730 ± 500	39 ± 5
Reacted dust	650 ± 40	12 ± 1	980 ± 80	7 ± 1	250 ± 40	3 ± 1
Biomass burning	540 ± 200	10 ± 4	3890 ± 600	28 ± 4	3170 ± 490	33 ± 5
Sea salt	2260 ± 330	43 ± 6	1740 ± 440	13 ± 3	1420 ± 380	15 ± 4
Heavy oil combustion	1110 ± 150	21 ± 3	1470 ± 410	11 ± 4	910 ± 410	10 ± 4

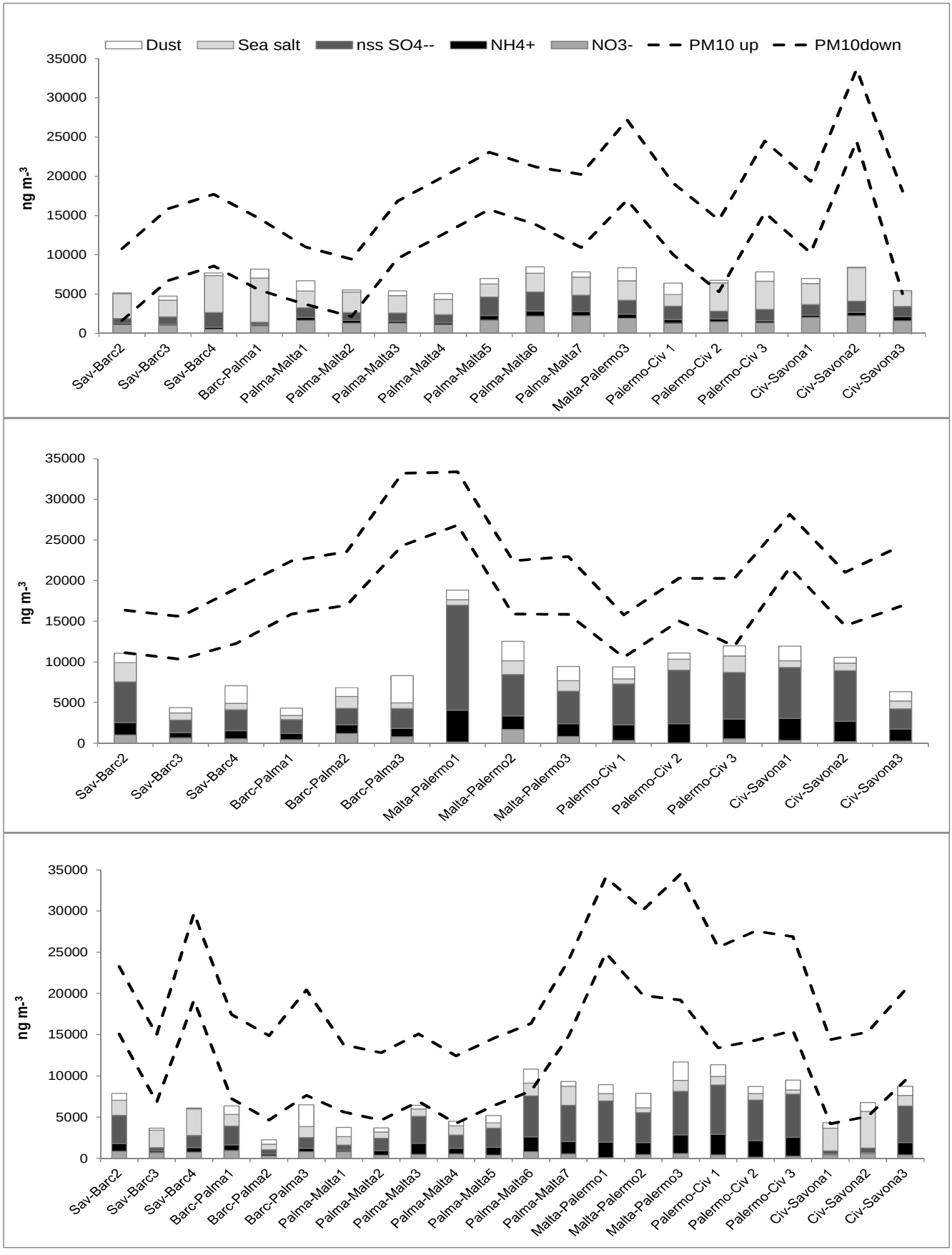
Dust
Sea salt
nss SO4--
NH4+
NO3-
PM10 up
PM10down
ng m-3
35000
30000
25000
20000
15000
10000
5000
0
Sav-Barc2
Sav-Barc3
Sav-Barc4
Barc-Palma1
Palma-Malta1
Palma-Malta2
Palma-Malta3
Palma-Malta4
Palma-Malta5
Palma-Malta6
Palma-Malta7
Malta-Palermo3
Palermo-Civ 1
Palermo-Civ 2
Palermo-Civ 3
Civ-Savona1
Civ-Savona2
Civ-Savona3
ng m-3
35000
30000
25000
20000
15000
10000
5000
0
Sav-Barc2
Sav-Barc3
Sav-Barc4
Barc-Palma1
Barc-Palma2
Barc-Palma3
Malta-Palermo1
Malta-Palermo2
Malta-Palermo3
Palermo-Civ 1
Palermo-Civ 2
Palermo-Civ 3
Civ-Savona1
Civ-Savona2
Civ-Savona3
ng m-3
35000
30000
25000
20000
15000
10000
5000
0
Sav-Barc2
Sav-Barc3
Sav-Barc4
Barc-Palma1
Barc-Palma2
Barc-Palma3
Palma-Malta1
Palma-Malta2
Palma-Malta3
Palma-Malta4
Palma-Malta5
Palma-Malta6
Palma-Malta7
Malta-Palermo1
Malta-Palermo2
Malta-Palermo3
Palermo-Civ 1
Palermo-Civ 2
Palermo-Civ 3
Civ-Savona1
Civ-Savona2
Civ-Savona3

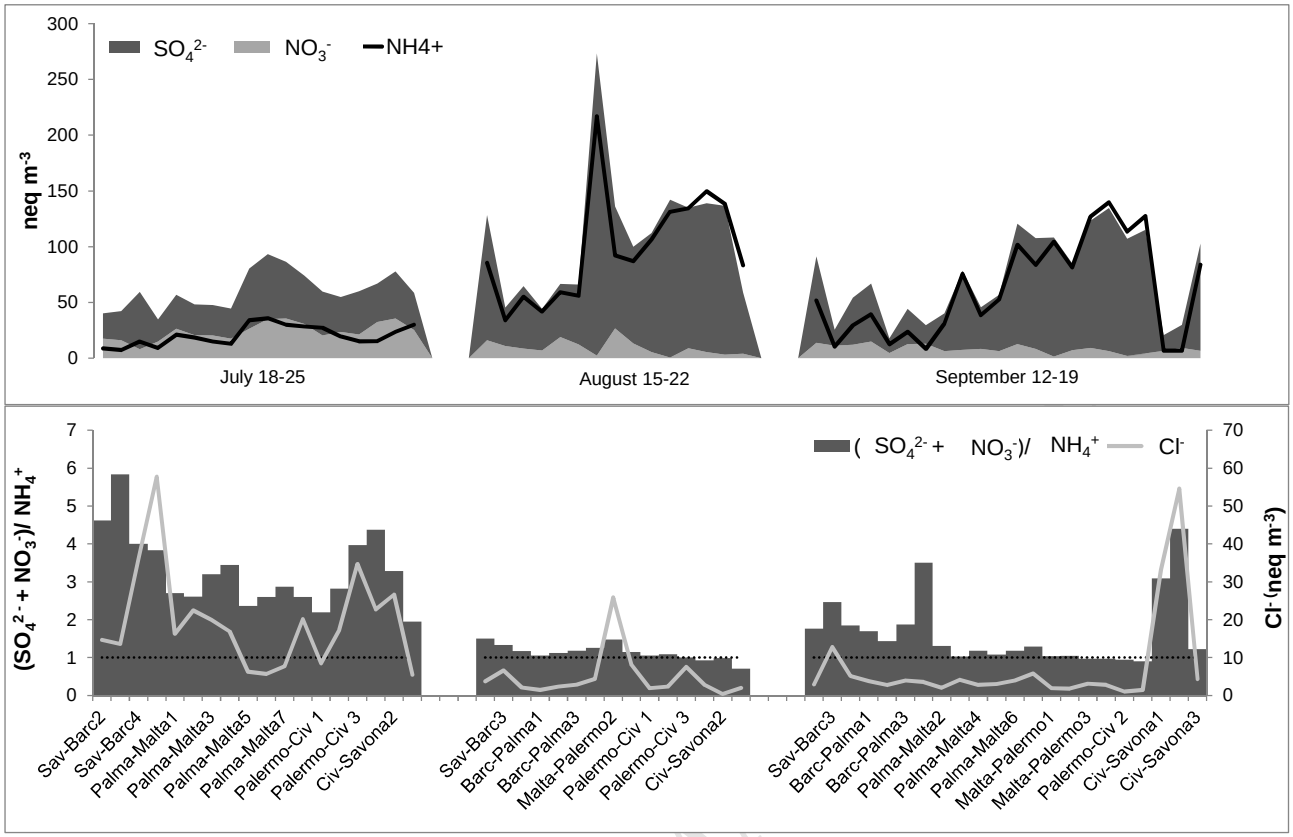

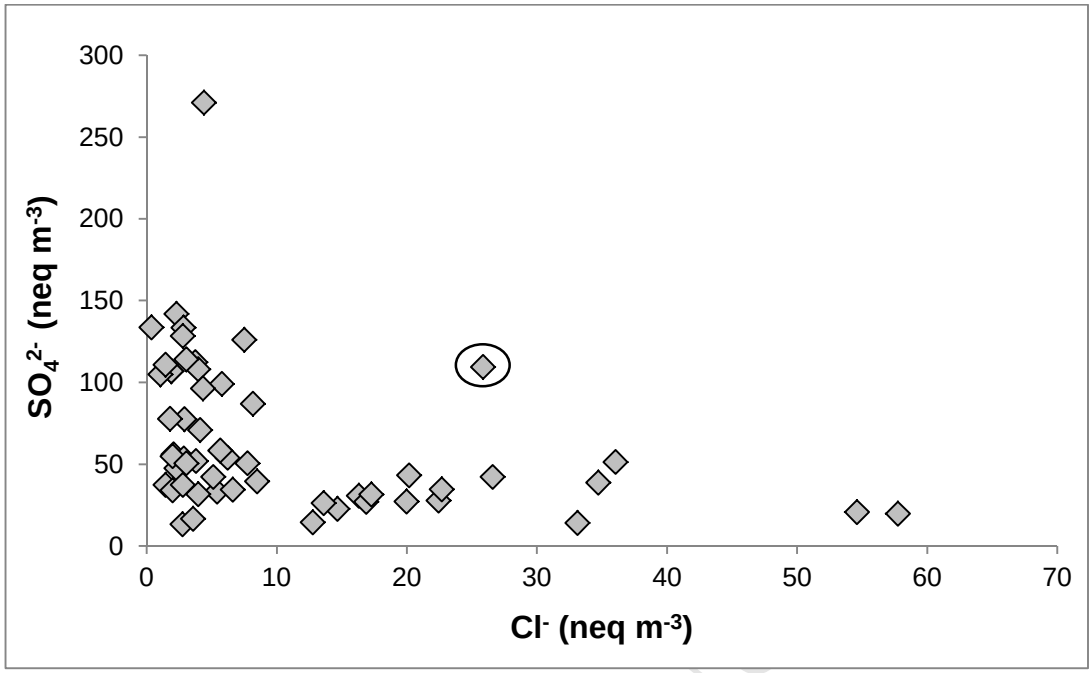

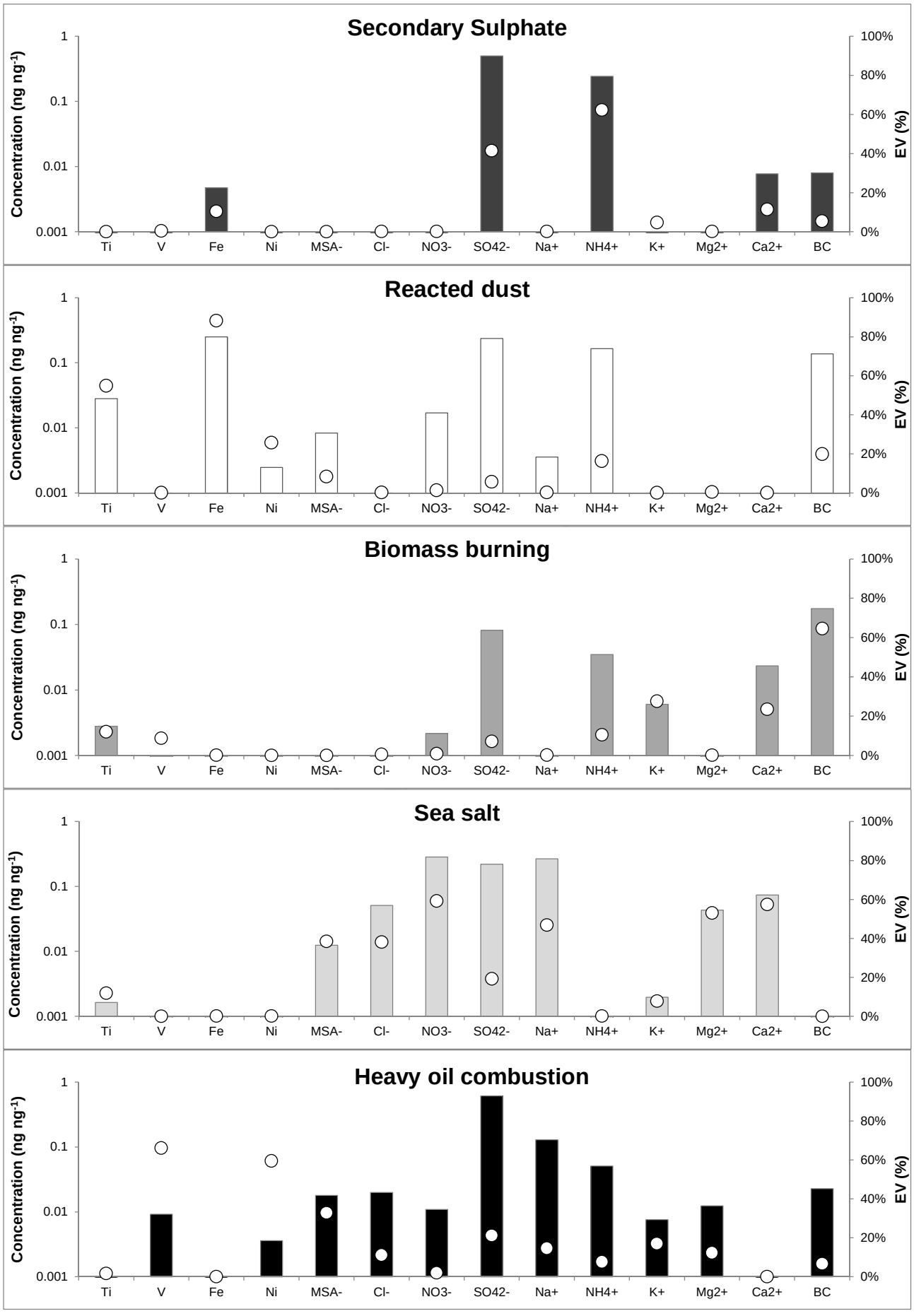
Secondary Sulphate
Reacted dust
Biomass burning
Sea salt
Heavy oil combustion
Concentration (ng ng-1)
EV (%)
1
0.1
0.01
0.001
100%
80%
60%
40%
20%
0%
Ti
V
Fe
Ni
MSA-
Cl-
NO3-
SO42-
Na+
NH4+
K+
Mg2+
Ca2+
BC

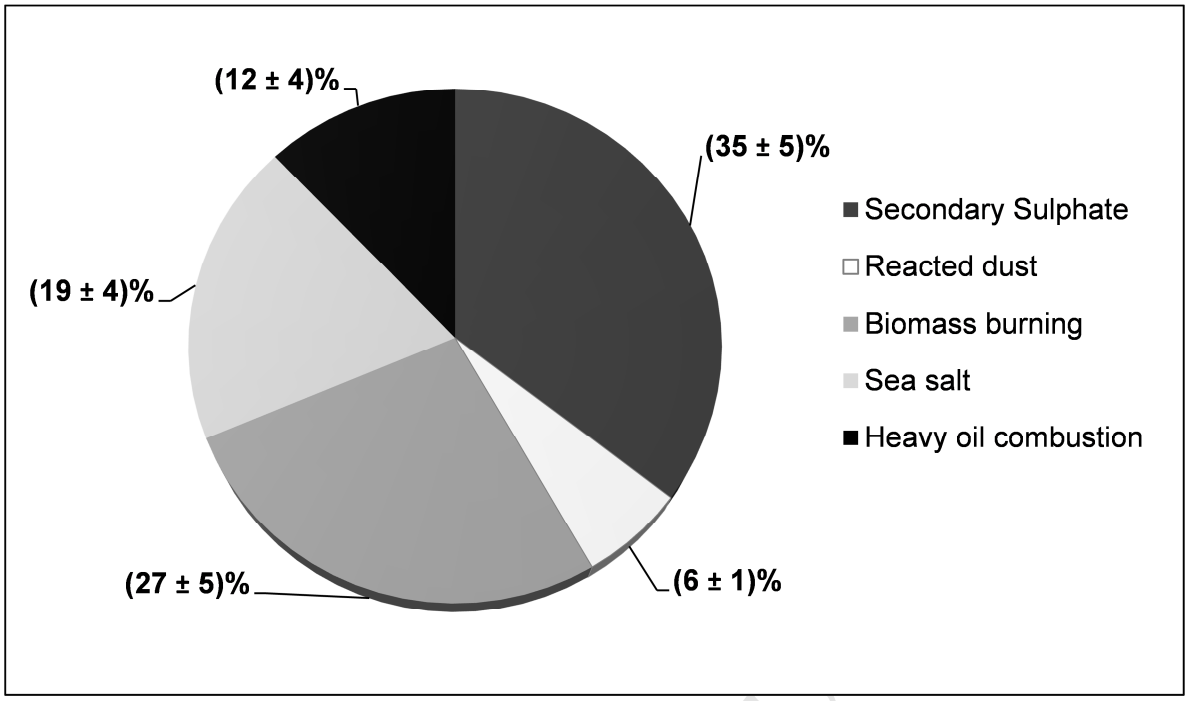

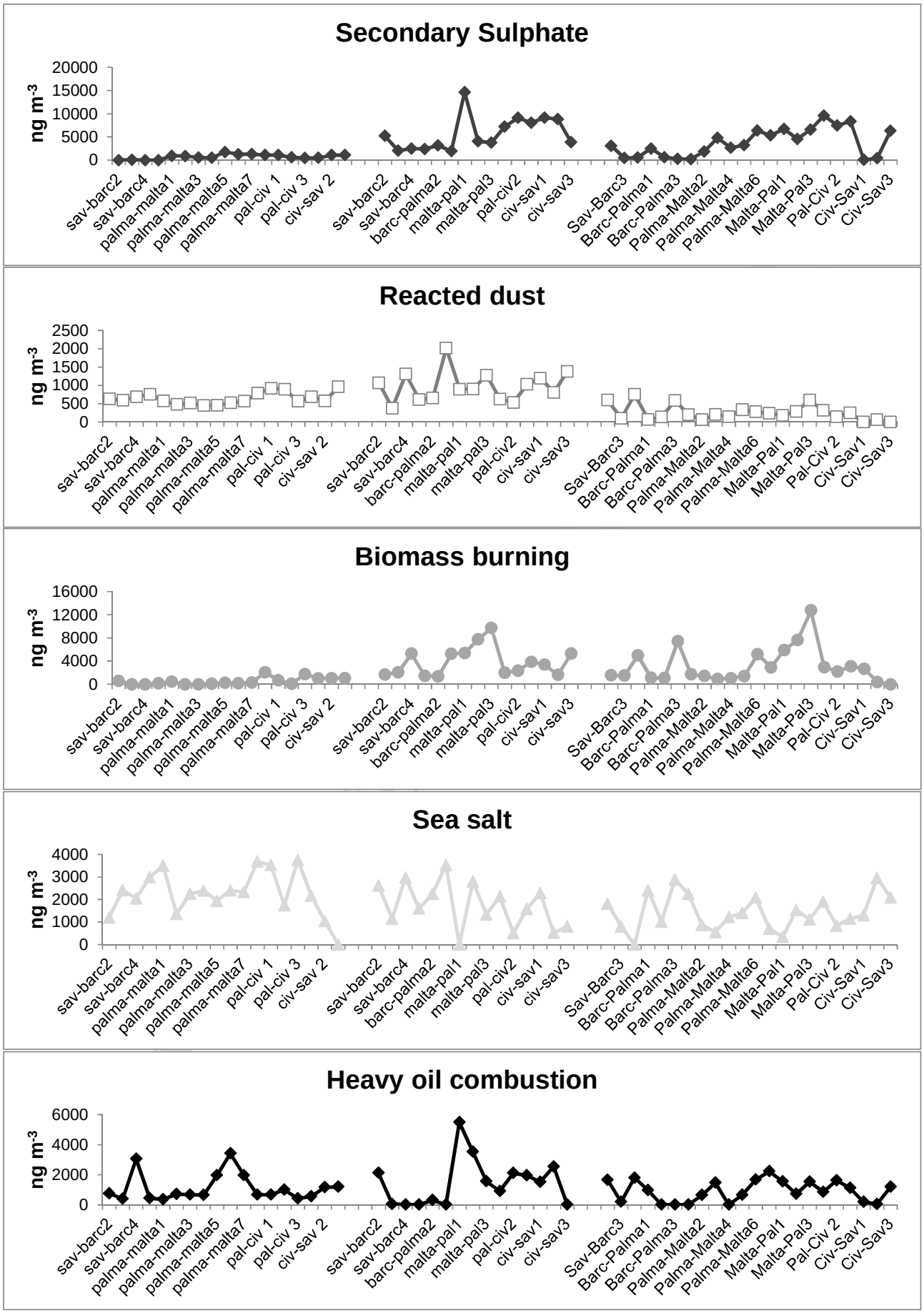
Secondary Sulphate
ng m-3
20000
15000
10000
5000
0
Reacted dust
2500
2000
1500
1000
500
0
Biomass burning
16000
12000
8000
4000
0
Sea salt
4000
3000
2000
1000
0
Heavy oil combustion
6000
4000
2000
0
sav-barc2
sav-barc4
palma-malta1
palma-malta3
palma-malta5
palma-malta7
pal-civ 1
pal-civ 3
civ-sav 2
barc-palma2
malta-pal1
malta-pal3
pal-civ2
civ-sav1
civ-sav3
Sav-Barc3
Barc-Palma1
Barc-Palma3
Palma-Malta2
Palma-Malta4
Palma-Malta6
Malta-Pal1
Malta-Pal3
Pal-Civ 2
Civ-Sav1
Civ-Sav3

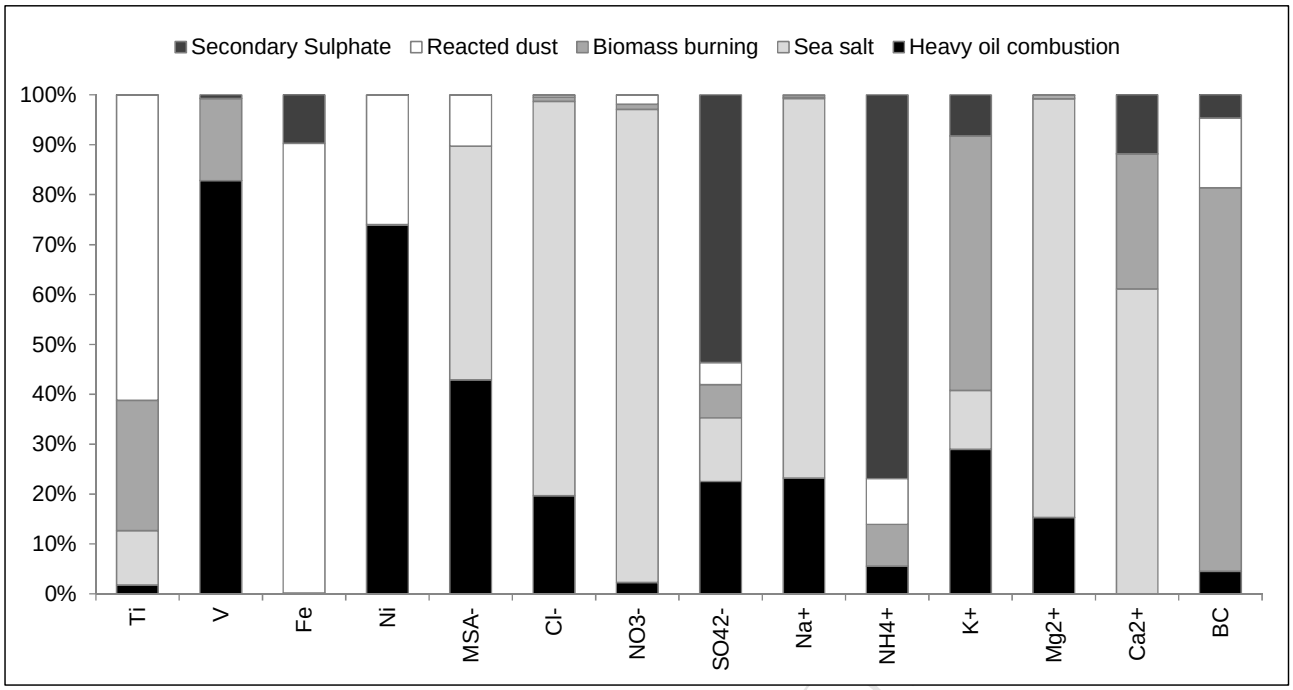

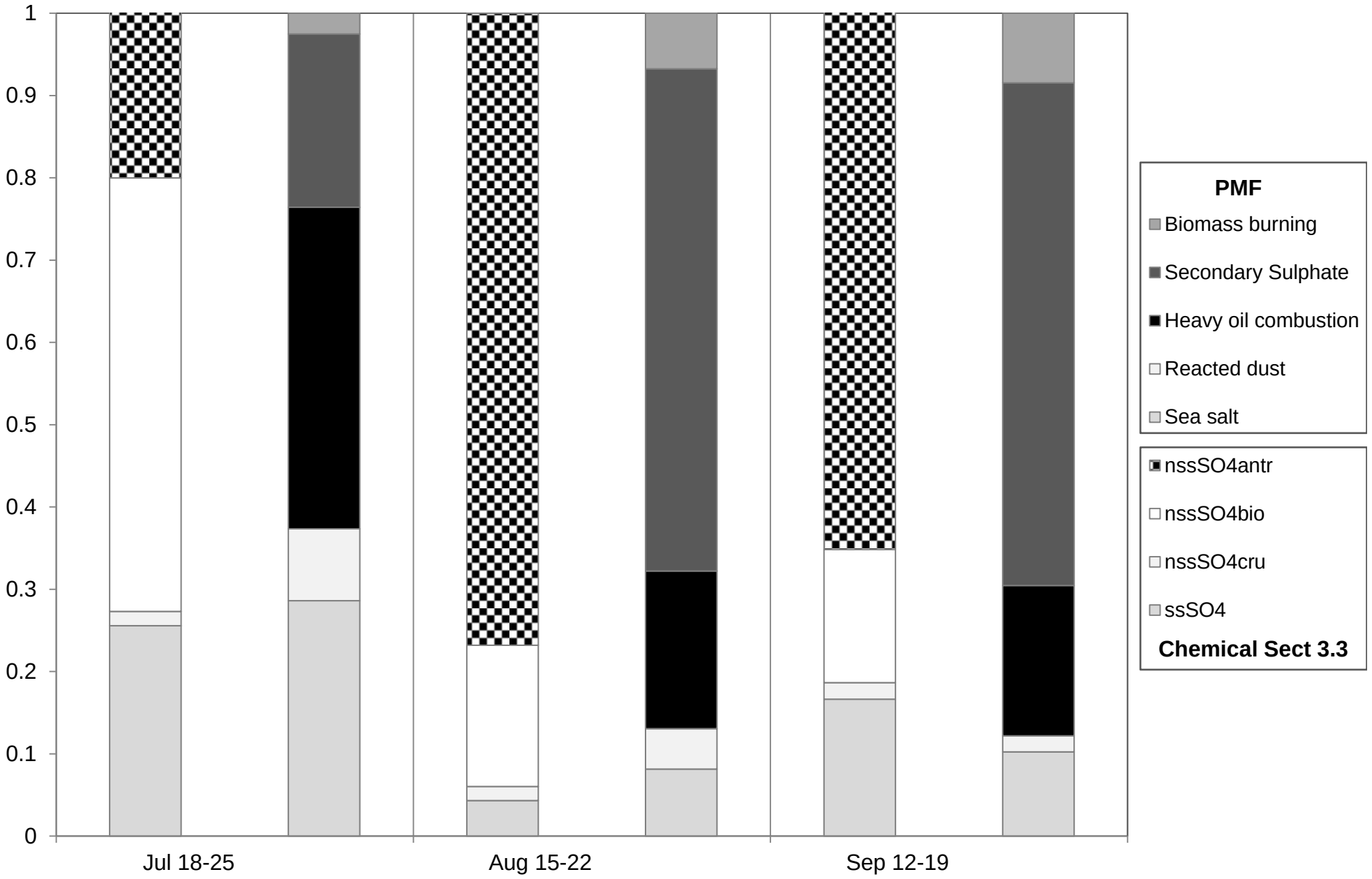
1
0.9
0.8
0.7
0.6
0.5
0.4
0.3
0.2
0.1
0
Jul 18-25
Aug 15-22
Sep 12-19
PMF
Biomass burning
Secondary Sulphate
Heavy oil combustion
Reacted dust
Sea salt
nssSO4antr
nssSO4bio
nssSO4cru
ssSO4
Chemical Sect 3.3

HIGHLIGHTS

- A conclusive PM10 sampling campaign on a cruise ship was performed in summer 2011
- PMF analysis allowed evaluating the main PM10 sources met along the ship route
- Large marine biogenic sulphur production was identified as function of strong winds
- The study disentangles primary ship emissions and secondary sulphates
- Primary ship emissions contributed on average to (12 ± 4)% of PM10